

BBA 73362

Characterization of eosin 5-isothiocyanate binding site in band 3 protein of the human erythrocyte

Tadahiko Chiba, Yukio Sato and Yasuo Suzuki

Pharmaceutical Institute, Tohoku University, Aobayama, Sendai (Japan)

(Received 28 April 1986)

(Revised manuscript received 22 October 1986)

Key words: Band 3; Anion transport; Competitive inhibition; Circular dichroism;
pH titration; Binding site; Erythrocyte membrane

The characteristics of the anion transport system in human erythrocyte, which can be modified by eosin 5-isothiocyanate (EITC), were studied using the pH titration method and by measuring the sulfate efflux. Based on the pH dependence of EITC binding to the erythrocyte ghosts, it was found that the reaction rate was maximal at about pH 6.4, and that the pH profile of EITC binding was similar to that of divalent anion transport. The interaction between EITC and ghosts was interpreted by a two-step reaction, a fast ionic-binding reaction and a slow covalent-binding reaction. The induced CD spectrum of the EITC-ghost system was also dependent on pH. The intensity of the CD band at 530 nm was decreased in acidic pH region, and the inflection point was observed at about pH 6.3, indicating a participation of the histidine residue in the interaction of EITC with band 3. In order to characterize the EITC-binding site, the kinetics of sulfate efflux in intact and EITC-modified cells were examined at various pH values. The inhibitory effect of EITC was dependent on pH. From the experimental results, the followings are suggested. (1) The rate of ionic interaction in the early stage is much slower than that in a general ionic reaction. A conformational change may participate in the reaction. (2) The conformation of the EITC-binding site depends on pH, relating to the dissociation of the histidine residues. (3) The EITC molecules act also as a competitive inhibitor to the sulfate efflux after binding covalently to band 3 protein.

Introduction

Band 3 is a major integral membrane protein of the human erythrocyte and its molecular weight is about 95 kDa [1]. The protein exists as a dimer and/or a tetramer under physiological conditions [2–4], and controls chloride-bicarbonate exchange

(see Refs. 5–10, for review). Sulfate [11], phosphate [12], and organic anionic compounds of low molecular weight [13] in addition to halide [14] are also transported by band 3 protein [9].

However, the pH dependence of the transport of monovalent anions is different from that of divalent anions [6]. The optimum pH for chloride transport is about 8.0, whereas that for sulfate is around 6.0 [11,16]. Milanick and Gunn [16] indicated that proton-sulfate co-transport is faster than sulfate transport alone, and that the optimum pH for the co-transport is 5.9. From the pH dependence of the anion transport, it is postulated that a positive group in the anion binding site is a

Abbreviations: DIDS, 4,4'-diisothiocyanostilbene-2,2'-disulfonate; EITC, eosin 5-isothiocyanate; H₂DIDS, 4,4'-diisothiocyanodihydrostilbene-2,2'-disulfonate; NAP-taurine, 2-[N-(4-azido-2-nitrophenylamino)]ethanesulfonate.

Correspondence: Y. Sato, Pharmaceutical Institute, Tohoku University, Aobayama, Sendai 980, Japan.

guanidino group of arginine. Matsuyama et al. [17] indicated that the optimum pH for the transport of inorganic phosphate and phosphoenolpyruvate are 6.5 and 6.8, respectively, and they suggested that a dissociation of imidazole group of histidine participates in these transport.

We also reported previously that eosin 5-isothiocyanate (EITC), an anion transport inhibitor [18], binds to the imidazole group of histidine in band 3 with ionic interaction [19], and that the histidine residues participate in the anion transport system of human red cells. EITC molecules are bound to band 3 proteins with 1:1 stoichiometry [20]. The binding site of EITC is different from that of 4,4'-diisothiocyanostilbene 2,2'-disulfonate (DIDS), which is also another typical anion transport inhibitor. However, a kinetic study of the EITC-band 3 complex has not been clear yet.

The present paper describes the pH dependence of the interaction of EITC with band 3 and the effects of EITC binding on the anion exchange.

Materials and Methods

Materials

Eosin 5-isothiocyanate (EITC) was prepared by bromination of fluorescein isothiocyanate according to the procedure of Cherry et al. [21]. Mes, Hepes, TAPS, CHES, and CAPS, that are called as Good's reagent [22] were obtained from Dojindo Laboratories. [^{35}S]Na₂SO₄ was purchased from Amersham. Other chemicals were of analytical reagent grade.

Preparation of ghosts

Fresh human red blood cells (treated by sodium citrate anti-coagulant) were obtained from Miyagi Prefectural Red Cross Blood Center. Human erythrocyte ghosts were prepared according to the procedure of Dodge et al. [23]. All operations were carried out at 0–4°C. Leaky ghosts were resealed in isotonic buffers with various pH values as shown in Table I.

Spectral measurements

The absorbance and circular dichroism (CD) spectra were taken with a Hitachi 220 spectrophotometer and a Jasco J-400X spectropolarimeter

TABLE I

LIST OF BUFFERS USED

The pH values were adjusted to the indicated values by addition of KOH. Abbreviations: Mes, 2-(*N*-morpholino)ethanesulfonic acid; Hepes, *N*-2-hydroxyethylpiperazine-*N'*-2-ethanesulfonic acid; TAPS, *N*-tris(hydroxymethyl)-3-aminopropanesulfonic acid; CHES, 2-(cyclohexylamino)ethanesulfonic acid; CAPS, 3-cyclohexylaminopropanesulfonic acid.

pH	Buffer's ingredient
5.0	5 mM Mes, 150 mM KCl
5.5	5 mM Mes, 150 mM KCl
6.0	5 mM Mes, 150 mM KCl
6.25	5 mM Mes, 150 mM KCl
6.5	5 mM Mes, 150 mM KCl
6.75	5 mM Mes, 150 mM KCl
7.0	5 mM Hepes, 150 mM KCl
7.5	5 mM Hepes, 150 mM KCl
8.0	5 mM TAPS, 150 mM KCl
8.5	5 mM TAPS, 150 mM KCl
9.0	5 mM CHES, 150 mM KCl
9.5	5 mM CHES, 150 mM KCl
10.0	5 mM CAPS, 150 mM KCl

equipped with a data processor, respectively. The absorbance difference spectra were measured using parallel cells of 5 mm pathlength. The measurements were carried out at 37°C.

The EITC-binding reaction to ghosts was monitored by the absorbance intensity at 540 nm in the difference spectra. The molar absorption coefficient, ϵ , was calculated on the basis of the initial concentration of EITC. The CD spectra of EITC were measured after incubation of EITC with ghost at 37°C for 2 h in the dark. The concentrations of protein in ghosts were determined by the method of Lowry et al. [24] using bovine serum albumin as standard. The concentrations of ghost protein and EITC were adjusted to 0.13 mg/ml and $1 \cdot 10^{-5}$ M, respectively.

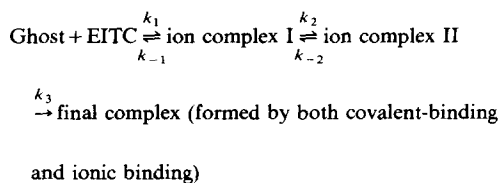
Sulfate efflux

Intact erythrocytes were washed twice with isotonic phosphate-buffered KCl solution (pH 7.4) and once with appropriate buffer in Table I. These cells were equilibrated at 37°C in the same medium for 2 h. They were washed and resuspended in the same medium to 10% hematocrit, [^{35}S]Na₂SO₄ added (1 $\mu\text{Ci/ml}$), followed by

incubation for another 2 h. These radioisotope loaded cells were added with various concentration of EITC and incubated for appropriated period at 37°C. In order to remove extracellular tracer and unreacted EITC, the cells were washed three times with the ice-cold buffer. Sulfate efflux was started by resuspending the cells at 5% hematocrit in the buffer at 37°C. After the incubation at 37°C, the radio activity was measured successively in deproteinized (2% trichloroacetic acid) cell supernatant.

Analysis of EITC binding to ghost

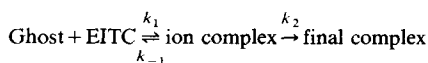
EITC has two anionic sites, which are the oxyo-anion at the xanthene skeleton and the carboxyl anion at the phenyl ring in the pH 5 to 10 region. The isothiocyano group at the phenyl ring is a covalent binding site. It is thought that EITC molecules are fixed on band 3 proteins by these three functional groups [19]. Although EITC molecules are also adsorbed slightly to the membrane, these EITC molecules have no influence on protein-binding kinetics [25]. Since the two anionic functional groups are not equivalent, the binding reaction of EITC molecules to ghosts is not simple. In general, an anionic interaction should be momentary and reversible. On the other hand, the amount of complexes formed by the covalent-binding reaction strongly depends on time. In the present study, it seems that its contribution to early stage in the reaction can be negligible. Thus, the reaction process can be presented by Scheme I.



Scheme I.

where k_1 , k_{-1} , k_2 , k_{-2} , and k_3 are rate constants, and ion complexes I and II indicate the EITC-ghost complexes formed by one and two ionic bonds, respectively. Since the complexes I and II are indistinguishable, we assume in this paper that the two ionic complexes are equivalent (Scheme

II).



Scheme II.

When the concentrations of ghost, EITC, ion complex, and final complex at time t are C_g , C_e , C_x , and C_y , respectively, the reaction process is described by the following coupled equations

$$\frac{dC_x}{dt} = k_1 \cdot C_e \cdot C_g - (k_{-1} + k_2) \cdot C_x \quad (1)$$

$$\frac{dC_y}{dt} = k_2 \cdot C_x \quad (2)$$

The initial concentrations of ghosts and EITC are C_{g0} and C_{e0} , respectively. When the concentration of EITC is much higher than that of band 3, C_e is nearly equal to C_{e0} .

Under this condition, we obtain

$$C_x = \frac{k_1 \cdot C_{e0} \cdot C_{g0}}{\rho_1 - \rho_2} (-e^{-\rho_1 t} + e^{-\rho_2 t}) \quad (3)$$

$$C_y = \left(1 + \frac{\rho_2}{\rho_1 - \rho_2} e^{-\rho_1 t} - \frac{\rho_1}{\rho_1 - \rho_2} e^{-\rho_2 t}\right) C_{g0} \quad (4)$$

where

$$\rho_1 = \frac{1}{2} \left(k_1 \cdot C_{e0} + k_{-1} + k_2 + \sqrt{(k_1 \cdot C_{e0} + k_{-1} + k_2)^2 - 4k_1 \cdot k_2 \cdot C_{e0}} \right)$$

and

$$\rho_2 = \frac{1}{2} \left(k_1 \cdot C_{e0} + k_{-1} + k_2 - \sqrt{(k_1 \cdot C_{e0} + k_{-1} + k_2)^2 - 4k_1 \cdot k_2 \cdot C_{e0}} \right)$$

When the molar absorption coefficients of EITC and ghosts are ϵ_e and ϵ_g , respectively, the intensity of the difference spectrum, ΔA , at time t is as follows, assuming that ϵ_g is constant before and after the reaction

$$\Delta A = a \cdot \epsilon_e (C_x + C_y) - \epsilon_e \quad (5)$$

where a is a proportionality constant.

We analysed the difference spectra using Eqn. 5. Data analyses were done by a non-linear least-

square method using a micro computer. In this study, the kinetic characteristics of the binding reaction were estimated by k_m or $\epsilon_e \cdot C_{e0} \cdot k_m$, where $k_m = k_1 / (k_{-1} + k_2)$.

Results

pH dependence of EITC binding to ghosts

The absorbance spectrum of EITC shows a main band at about 522 nm and a shoulder at about 483 nm. When EITC molecules are bound to ghosts, the absorbance maximum shifts to about 525 nm with a decrease in intensity [25]. A difference spectrum between EITC-ghost complexes and free EITC shows a positive peak at about 540 nm and two negative peaks at about 516 nm and 483 nm at pH 7.4. The pH effects on these peaks were examined (Fig. 1(a)). As pH increased, the intensities of three peaks decreased accompanied by shifts to shorter wavelengths (positive peak; 539 nm at pH 8, 542 nm at pH 6; strong negative peak; 515 nm at pH 8, 519 nm at pH 6). Fig. 1(b) shows the peak intensity of three bands as a function of pH. All of these pH profiles revealed inflection points at pH 6.4. We previously indi-

cated that the increase of these peaks in the rather long reaction time at pH 7.4 could be approximately interpreted by a first-order reaction and that the rate constants of the change for the three peaks were the same [25]. The behavior of these three peaks was the same at other pH. Thus, in the following experiments, the EITC-binding reaction to ghosts was monitored by the change at 540 nm.

Fig. 2(a) shows the time-courses of the EITC-binding reaction to ghosts at various pH values. It is obvious that the reaction strongly depends on the pH. Since EITC has two ionic-binding groups and one covalent-binding group, the binding reaction of EITC to ghosts consists of the fast ionic-binding reaction and the slow covalent-binding reaction. In general, the ionic reaction is so fast that the reaction is approximated by the pseudo-first-order reaction, $y = a_1 + a_2(1 - \exp(-kt))$. However, the absorbance change in the EITC-ghost system cannot be fitted well by this equation. Thus, we analyzed the difference spectra using Eqn. 5, described in Materials and Methods. The reaction curves shown in Fig. 2(a) could be explained well by this equation in all pH regions. This means that the ionic interaction in the

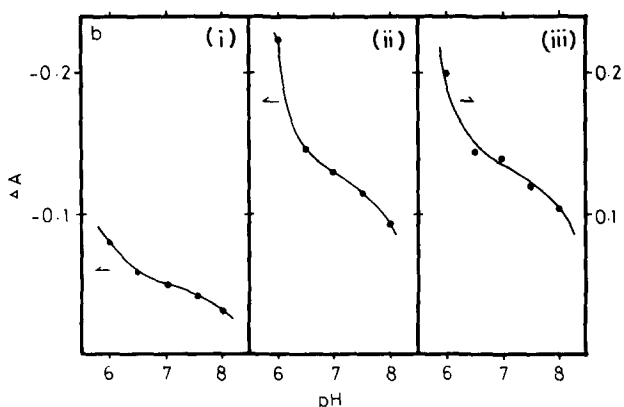
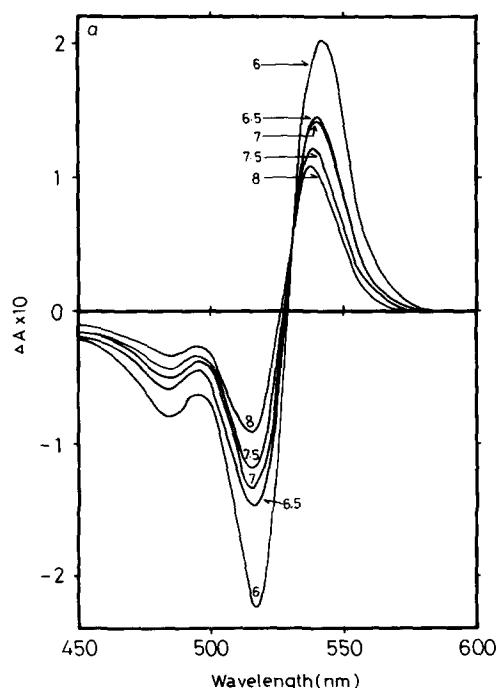


Fig. 1. (a) Difference spectra of EITC-ghost system at various pH values. [EITC], $1 \cdot 10^{-5}$ M; [ghost], 0.13 mg protein/ml; path length, 5 mm. A mixture of EITC and ghosts was incubated for 2 h at 37°C in the dark. (b) pH dependence of the peak intensities of the difference spectra of EITC-ghost system. The peak intensities were taken from Fig. 1(a). (i) Negative peak at the shorter wavelength side; (ii) negative peak at the longer wavelength side; (iii) positive peak.

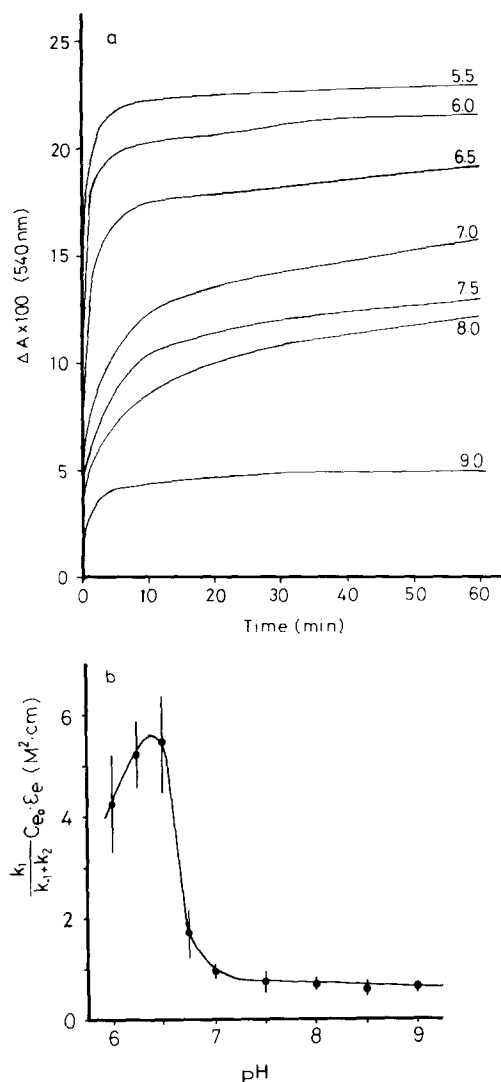


Fig. 2. (a) pH dependence of the time-course in the EITC-ghost reaction at 37°C. The numbers in the figure indicate the pH values. [EITC], $1 \cdot 10^{-5}$ M; [ghost], 0.13 mg protein/ml; path length, 5 mm. (b) pH profiles for the rate constant in the EITC-ghost reaction. For the details of the data analysis, see the text. Bars show the standard deviations for at least three determinations.

EITC-ghost system proceeds rather slowly, because a contribution of the first term in Eqn. 5 could not be neglected.

Fig. 2(b) shows the pH profile for k_m ; the values of $\epsilon_e \cdot C_{e0} \cdot k_m$ (ϵ_e and C_{e0} : constant) were plotted as a function of the pH. The values of k_m are rather large in the acidic region. The maximum value of k_m is obtained at a pH of about

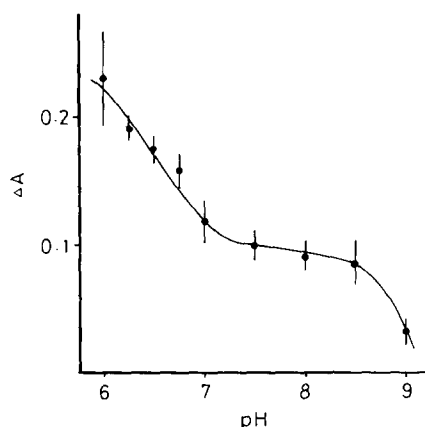


Fig. 3. pH dependence of the intensity of difference spectra at 540 nm in the EITC-ghost reaction. Data points were obtained by calculations using Eqn. 5, assuming that t is infinite. Bars show the standard deviations for at least three determinations.

6.4. The intensities of the difference spectra were calculated using Eqn. 5 at various pH values.

As shown in Fig. 3, the values of theoretical ΔA at 540 nm decreased with increasing pH. Two inflection points were revealed at about pH 6.4 and 8.7. This result is consistent with the previous experimental result, in which the curve of pH profile was plotted after 2 h incubation [19]. This incubation time may correspond to infinite time in Eqn. 5. In that case, new equilibria were revealed at pH 6.4 and 8.0.

pH dependence of the CD spectrum of the EITC-ghost system

Although EITC has a chirality due to steric hindrance of the carboxyl group on the phenyl ring, it is racemic and optically inactive when it is free in solution. It is known, however, that EITC molecules bound to ghosts show an induced CD resulting from a perturbation of the enantiomer distribution upon binding to band 3 [20]. As shown in Fig. 4(a), the induced CD spectrum has a positive band at about 530 nm and a shoulder at about 490 nm. Fig. 4(b) shows the pH dependence of CD intensity at 530 nm after 2 h incubation at various pH values. From this pH-equilibrium profile, an inflection point is revealed at about pH 6.3. When the EITC-ghost system was preincubated at pH 7.4 and then it was exposed to pH values from 5 to 10, a titration curve similar to the profile in Fig. 4(b) was obtained. It should be

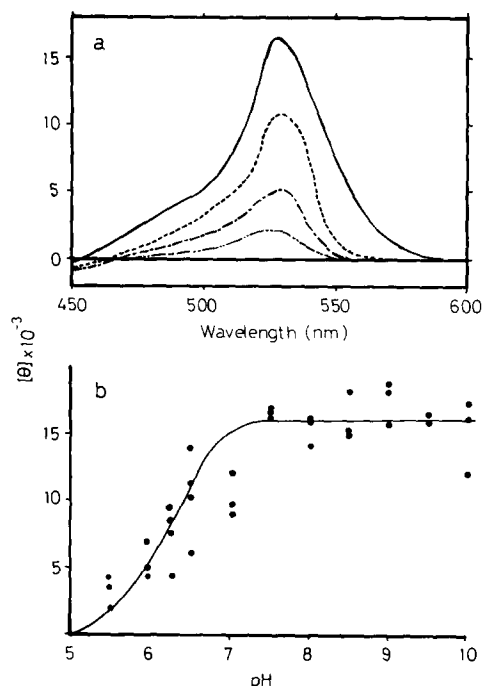


Fig. 4. (a) CD spectra of the EITC-ghost system incubated at various pH values. —, pH 7.5; — —, pH 6.5; ·····, pH 6; ·-·-·, pH 5.5, [EITC], $1 \cdot 10^{-5}$ M; [ghost], 0.13 mg protein/ml; path length, 1 cm. A mixture of EITC and ghosts was incubated for 2 h at 37°C in the dark. (b) pH dependence of the CD intensity at 530 nm in the EITC-ghost system. The experimental conditions were the same as those in Fig. 4(a).

noticed that the CD intensity remains almost unchanged from pH 7.5 up to pH 10. The covalent binding between EITC and band 3 protein is not affected by pH change. EITC exists in the dissociated form in the pH region from 5 to 10. Thus, the change of CD intensity should be due to the dissociation of the cationic amino acid residues in band 3 protein. In a previous report, it was proposed that the imidazole group of histidine and the guanizino group of arginine participate in the EITC binding to band 3 protein [19]. The guanizino group of arginine exists in the dissociated form in the weak acidic to alkaline regions. On the other hand, the imidazole group of histidine exists in a molecular form in the alkaline region. Therefore, it can be said that the change in CD intensity results from a variation in the interaction of EITC with the imidazole groups, reflecting the conformational change of the EITC-binding sites.

pH dependence of the inhibitory effect of EITC on sulfate efflux

Nigg et al. [18] showed that eosin derivatives inhibit sulfate transport in intact erythrocytes at pH 7.4. We examined the inhibitory effect of EITC on sulfate transport at several pH values from 6 to 8. Fig. 5 shows the concentration dependence of the inhibitory effect at various pH values. At pH 8, $2 \cdot 10^{-5}$ M EITC inhibited the sulfate transport by about 83%. Above pH 8, the inhibitory effect was similar to that at pH 8. At pH 7.5 and 7, however, the transport was inhibited by about 45% and 20%, respectively. Below pH 6.5, the sulfate transport was not apparently inhibited by EITC.

The inhibitory effect of EITC was also examined by changing the modification period at various pH values (Fig. 6). At pH 8, the maximum inhibition was reached after 2 h incubation. At pH 7.5, however, the inhibitory effect was insufficient even after 3 h incubation, and below pH 6.5, no inhibitory action of EITC was observed. At low pH, the transport was apparently enhanced by a short incubation time. This may suggest that, at the initial stage in the interaction, a local structure of the EITC-band 3 complex in the low-pH region is slightly different from that in the alkaline-pH

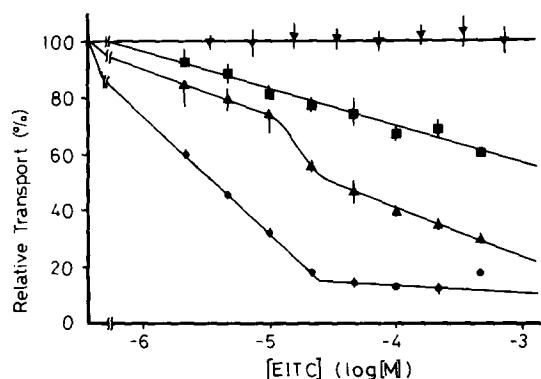


Fig. 5. Effect of the EITC concentration on sulfate efflux at various pH values. ▼, pH 6.5; ■, pH 7; ▲, pH 7.5; ●, pH 8. Bars show the standard deviation for at least three determinations. ^{35}S -labelled erythrocytes were allowed to react with various concentrations of EITC for 2 h at 37°C , and then washed three times to remove excess isotope and EITC. The sulfate effluxes were measured using deproteinized cell supernatant after further incubation for 2 h at 37°C . Erythrocyte concentration, 5% hematocrit. Relative transport = (the count in supernatant of EITC-modified cell)/(the count in supernatant of intact cell).

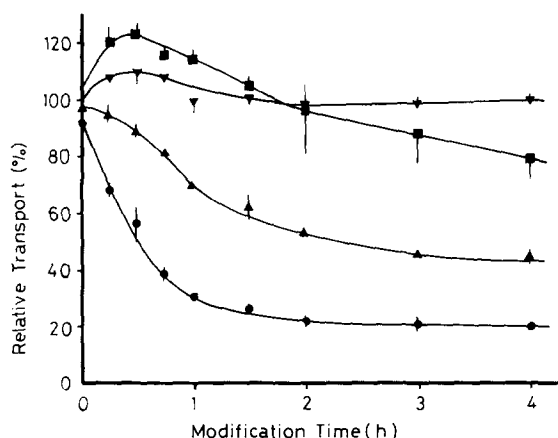


Fig. 6. Effect of EITC-modification time on sulfate efflux at various pH values. ▼, pH 6.5; ■, pH 7; ▲, pH 7.5; ●, pH 8. Bars show the standard deviations from three determinations. ^{35}S -labelled erythrocytes were allowed to react with $5 \cdot 10^{-5}$ M EITC for various modification periods at 37°C , and then washed three times with 10 volumes of the ice-cold buffer. The sulfate effluxes from the EITC-modified cells were measured using deproteinized cell supernatant after further incubation for 2 h at 37°C in the same buffer. Control cells were prepared by adding buffer instead of EITC. Erythrocyte concentration, 5% hematocrit. Relative transport = (the count in supernatant of EITC-modified cell)/(the count in supernatant of the control cell).

TABLE II

KINETICAL PARAMETER OF THE SULFATE EFFLUX

^{35}S -labelled erythrocytes were reacted with $5 \cdot 10^{-5}$ M EITC for 2 h at 37°C , and then washed three times with the 10 volumes of ice-cold buffer. The EITC-bound cells were incubated in the same buffer for several hours at 37°C . After centrifugation and deproteinization, the radioactivity of supernatant was measured. Initial rate of transport, k , were calculated by the following equation:

$$kt = \ln(m/(m - x)),$$

where x and m are the radioactivity in the supernatant at time t and at the equilibrium condition, respectively.

pH	Rate coefficient of sulfate self-exchange (min^{-1})		Ratio k_e/k_c
	control cells (k_c)	EITC-modified cells (k_e)	
6.0	0.0376	0.0431	1.146
6.5	0.0421	0.0272	0.647
7.0	0.0322	0.0142	0.441
7.5	0.0171	0.00445	0.261
8.0	0.0117	0.00280	0.239

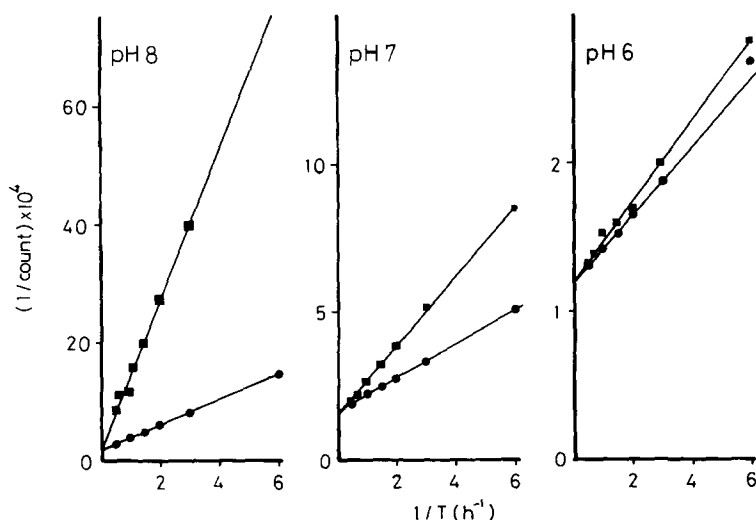


Fig. 7. Double-reciprocal plots of sulfate effluxed and time. ●, control cells; ■, EITC-treated cells. ^{35}S -labelled erythrocytes were allowed to react with $5 \cdot 10^{-5}$ M EITC for 2 h at 37°C , and then washed three times with 10 volumes of ice-cold buffer. The EITC-modified cells were incubated in the same buffer at 37°C . The isotope content was measured after appropriate incubation periods. The control cells were prepared by adding buffer instead of EITC. The isotope content was measured as described above. Erythrocyte concentration, 5% hematocrit. The regression lines were determined by the smallest mean square method. The y -intercepts of control cells at pH 6, 7, and 8 are $1.198 \cdot 10^{-4}$, $1.639 \cdot 10^{-4}$, and $2.006 \cdot 10^{-4}$, respectively, and those of EITC-modified cells at pH 6, 7, and 8 are $1.192 \cdot 10^{-4}$, $1.552 \cdot 10^{-4}$, and $2.030 \cdot 10^{-4}$, respectively.

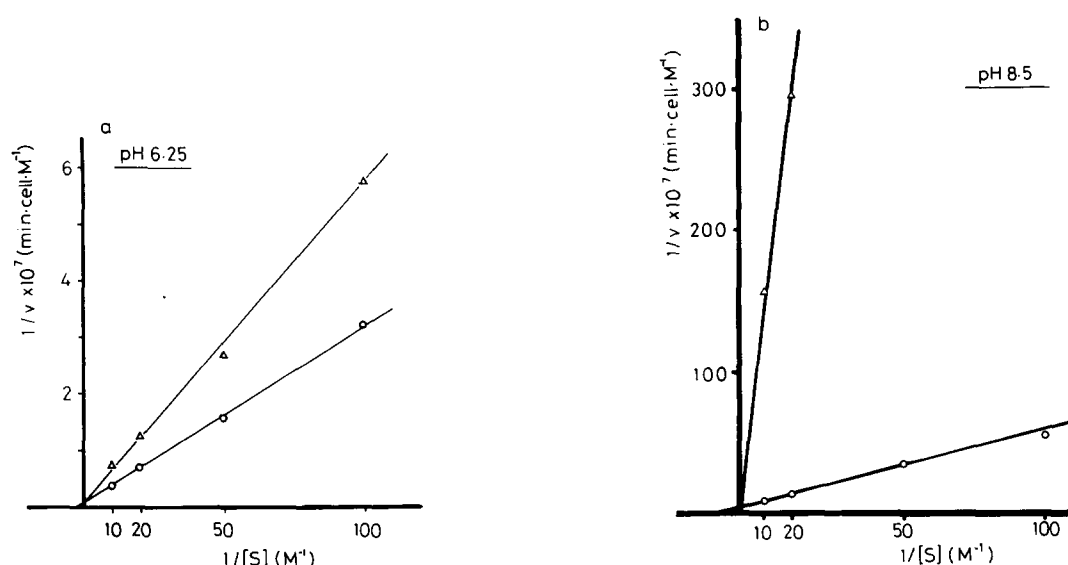


Fig. 8. Lineweaver-Burk plots of sulfate efflux for intact and EITC-modified cells at pH 6.25 and 8.5. \circ , intact cells; Δ , EITC-modified cells. The conditions of EITC modification and sulfate efflux were the same as those in Fig. 7. Initial transport rate, k , and sulfate efflux, V , were calculated by the following equations:

$$kt = \ln(m/(m - x)) \quad \text{and} \quad V = kn$$

where x and m are the radioactivity in supernatant at time t and at the equilibrium condition, respectively. n is a concentration of substrate, sodium sulfate. Erythrocyte concentration, 5% hematocrit. The regression lines were determined by the smallest mean square methods. The y -intercepts of control and EITC-modified cells at pH 6.25 are $0.00725 \cdot 10^{-7}$ and $0.0114 \cdot 10^{-7}$, respectively, and those at pH 8 are $6.337 \cdot 10^{-7}$ and $9.899 \cdot 10^{-7}$, respectively.

region. The detail, however, is unknown.

These results suggest that the inactivation of transport by EITC is dependent on the concentration of EITC and on the modification time. Furthermore, it is likely that both reversible and irreversible inhibitions take part in the interaction of EITC with band 3 protein. This corresponds to the analytical data in Fig. 2(b), in which the interaction was explained by two reactions, ionic binding and covalent binding. Then we compared the sulfate-efflux rate in intact erythrocytes with that of EITC-treated erythrocytes at various pH values. The results are shown in Table II. The rate constants, k_e for the EITC-modified erythrocytes and k_c for the intact erythrocytes, decrease with increasing pH. However, the degree of decrease of k_e is greater than that of k_c as indicated by the k_e/k_c value.

Although the inhibitory effect was observed at pH 6.5 (Table II), the result in Fig. 5 did not coincide with its inhibition at the same pH. It is

likely that the inhibitory effect at pH 6.5 is competitive. Double-reciprocal plots of $^{35}\text{SO}_4^{2-}$ transport and time are shown in Fig. 7. The regression lines of the EITC-treated and intact systems intersected at the same positions on the vertical at each pH. Similar results were observed at pH 6.25, 6.5 and 7.5 (data not shown). It can therefore be presumed that EITC molecules act as competitive inhibitors for the sulfate efflux at the pH regions studied. To examine this possibility, the effect of EITC on sulfate efflux was measured at different sulfate concentrations. Fig. 8 shows a Lineweaver-Burk plot of the characteristics of the inhibition by EITC at pH 6.25 and 8.5. The pattern of inhibition is better characterized as competitive with respect to the sulfate efflux. This indicates that the ionic component in the EITC-band 3 interaction participates in the anion transport with a partial inhibitory effect. Such a property is not observed in covalent-binding stilbenedisulfonate derivatives such as DIDS or H_2DIDS .

Discussion

Binding reaction of EITC to band 3 protein

As shown in Scheme I, the binding reaction is composed of three processes, two ionic-binding reactions and a covalent-binding reaction. It should be approximated as pseudo-first-order reaction, because generally the ionic-binding reaction occurs so rapidly. Lepke et al. [26] showed that H_2DIDS binds covalently to band 3 protein with pseudo-first-order kinetics, and that a non-covalent reaction of H_2DIDS is achieved in a moment. It is well known that a binding site of H_2DIDS is a 'substrate site' faced extracellular [27]. In the present study, it is found that the fast-phase reaction is much slower than a general ionic reaction. Thus, it is considered that the charged groups for the EITC-binding do not expose directly to the EITC molecules.

Brauer et al. [28] measured phosphate-chloride exchange in human erythrocytes using ^{31}P - and ^{35}Cl -NMR. They analyzed the anion transport in terms of a mobile carrier (lock in) model, in which the anion-binding site exposes to the extra- or intra-cellular solvent. Thus, it can be considered that a time-course of the anion exchange is also composed of two phases. We found that Eqn. 5 could be used well also to explain the experimental values in their literature using the P_i flux instead of ΔA . It is thought that anion exchange participates in the conformational change of band 3 protein [6,8]. Since the character of the binding reaction of EITC to band 3 is similar to the anion exchange, it is suggested that the EITC-binding reaction to band 3 in the fast phase should be accompanied by a conformational change of the protein.

pH-dependence of conformational change of band 3 protein

The binding reaction of EITC to band 3 progresses most effectively at about pH 6.4. The sulfate transport exhibits a pH maximum at about pH 6.2 [11,16]. In other words, the active pH is near the pH value at which the sulfate flux exhibits its maximum. This suggests that EITC molecules probably act as divalent anions in the reaction. We reported previously that EITC interacts with the imidazole group of histidine of band

3 with an ionic bond [19]. The histidine residue is a functional amino acid which participates in anion recognition or anion binding in the anion transport by band 3. Since the pK value of imidazole group is 6.0, the active pH may be related to the dissociation of histidine. However, in acidic pH region, the inhibitory action of EITC is small, implying that the EITC-binding activity is not correlated directly with the inhibitory effect. The magnitude of the CD spectra of the EITC-ghost complex decreases with decreasing pH (Fig. 4). Further, the result of the pH dependence of the CD intensity corresponds to that of the inhibitory effect of EITC (Table II). At the pH region where the strongest CD was observed, EITC inhibits anion exchange most effectively. Thus, in the EITC-ghost system, the CD intensity is proportional to the inhibitory effect. The pH of 6.4 may be critical for the CD and the inhibitory action of EITC. It seems that the topographic character of the functional amino acids at the alkaline pH region is favorable for EITC binding. The conformational change of the EITC-binding site accompanied by the pH change should be closely related to the dissociation of histidine.

The pH dependence of ΔA values shown in Fig. 3 exhibits two inflection points at pH 6.4 and 8.7. This reflects a change of electrostatic interaction between EITC and amino acid residues at the anion-recognition site in band 3. The equilibrium at pH 8.7 is not observed in the pH dependence of the CD intensity (Fig. 4(b)) and the inhibitory action of EITC. It is known that the H_2DIDS binding to band 3 proceeds in proportion to increasing pH [27,29]. Kampmann et al. [29] found that the binding activity of H_2DIDS is related to the dissociation of two lysine residues, which show different reactivities towards the isothiocyano groups of the H_2DIDS molecule. The dissociation constant of amino acid residue depends not only on the chemical nature of the dissociating group itself but also on the properties of the environment. Therefore, we cannot deny that the inflection point at pH 8.7 also corresponds to the dissociation of the lysine residue. When the pH of the EITC-ghost system was changed by adding HCl or NaOH after 2 h incubation at 37°C (pH 7.4), the inflection point was observed at pH 8.0 [19]. These discrepancies may result from the dif-

ference in the conformational environment which is dependent on the experimental conditions. At present, however, the details are unknown.

Characterization of EITC binding site

It is well known that there are at least two kinds of binding site for inhibitors in the transport system of band 3 protein [6–9]. One is a ‘substrate site’ and the other is a ‘inhibitorial modifier site’ [30]. Stilbene derivatives bind to the substrate site, and inhibit the anion transport [31–33]. On the other hand, Knauf et al. [34,35] indicated that NAP-taurine binds covalently or noncovalently to the modifier site. They suggested that the binding site of NAP-taurine exists on the exterior side of the cell rather than the substrate sites [34–36].

We reported previously some characteristics of the EITC-binding site as [19,20]. (1) The spatial arrangement of the functional amino acids in the EITC-binding site is different from that in the DIDS-binding site. (2) EITC binding is blocked by preincubation with DIDS, though DIDS binding is not blocked by preincubation with EITC. (3) Amino acid residues in the EITC-binding site are histidine, arginine, and, perhaps, lysine. In this study, the followings are revealed. (1) The kinetic character in the EITC-binding reaction resembles that in the divalent anion transport. (2) The conformation of the EITC-binding site depends on pH. (3) The EITC molecules inhibit sulfate efflux by competing. The competitive inhibition of EITC corresponds to the concept that internal NAP-taurine inhibits chloride fluxes by competing at a site with a chloride affinity similar to that of the substrate site [34]. On the other hand, the external NAP-taurine which acts at the modifier site shows a far more potent inhibitory effect on chloride exchange. In the previous report, we proposed that the EITC-binding site may be identical to the modifier site [25]. However, EITC seems to interact with the site which is not strictly identical to the modifier site for NAP-taurine. Therefore, it can be said that the EITC-binding site may be slightly different from that previously reported.

Character of the transport channel

Although several models have been proposed to explain the anion exchange mechanism catalyzed by band 3 protein [5,6,8], they can be classified

into two types that may be designated as ‘lock in’ and ‘zipper’ models [37]. The ‘lock in’ model postulates that there is only a single transport gate, which can exist in either an outward-facing form or an inward-facing form [38–42]. In this model, the tightly coupled one-for-one exchange of anions is explained by postulating that the interconversion from outward-facing form to inward-facing form or vice versa can only occur after binding of the anions to the substrate site. Wieth et al. [44] proposed a ‘zipper’ mechanism model. The zipper model postulated that there is an interlocking device set along two edges which can be separated and reunited, allowing anions to slide between them. The interlocking device set is postulated to consist of the salt bridges between functional amino acids. Knauf et al. [36,40] indicated that the transport system is asymmetric, because NAP-taurine or niflumic acid can bind to the extracellular site only. They suggested also that NAP-taurine and niflumic acid inhibit the anion exchange by blocking the conformational change of band 3 protein, though the binding sites of them differ from one another.

It has been proposed that lysine [45], histidine [17,18], arginine [46–52] residues, and carboxyl groups [53] are responsible for the anion transport. In this study, however, it seems that the lysine residue which binds covalently with EITC does not play an essential role in the anion transport, since sulfate efflux was observed in EITC-modified cells. Bjerrum et al. [48] suggested that there is an active arginine residue in the extracellular site. On the other hand, Zaki [51] reported that the arginine residues are exposed to the inner membrane surface. These results suggest that there are at least four domains which should be involved in transport activity and be composed of different functional amino acids. At present, the ‘zipper’ model seems to be adequate to explain the anion exchange mechanism because of the participation of more than one kind of amino acid residue in the anion transport. However, modifications for this model are required, because the role of many functional amino acids and their topographic characters have not become apparent yet. A study along this line is in progress.

References

- 1 Fairbanks, G., Steck, T.L. and Wallach, D.F.H. (1971) *Biochemistry* 10, 2606–2617
- 2 Wang, K. and Richards, F.M. (1975) *J. Biol. Chem.* 250, 6622–6626
- 3 Haest, C.W.M., Kamp, D., Plasa, G. and Deuticke, B. (1977) *Biochim. Biophys. Acta* 469, 226–230
- 4 Nigg, E. and Cherry, R.J. (1979) *Nature* 227, 493–494
- 5 Deuticke, B. (1977) *Rev. Physiol. Biochem. Pharmacol.* 78, 1–97
- 6 Cabantchik, Z.I., Knauf, P.A. and Rothstein, A. (1978) *Biochim. Biophys. Acta* 515, 239–302
- 7 Barzilay, M., Ship, S. and Cabantchik, Z.I. (1979) *Membrane Biochem.* 2, 227–254
- 8 Knauf, P.A. (1979) *Curr. Top. Membranes Transp.* 12, 249–363
- 9 Jennings, M.L. (1984) *J. Membrane Biol.* 80, 105–117
- 10 Jennings, M.L. (1985) *Annu. Rev. Physiol.* 47, 519–533
- 11 Schnell, K.F., Gerhardt, S. and Schöppe-Fredenberg, A. (1977) *J. Membrane Biol.* 30, 319–350
- 12 Ho, M.K. and Guidotti, G. (1975) *J. Biol. Chem.* 250, 675–683
- 13 Hamasaki, N., Matsuyama, H. and Hirota-Chigita, C. (1983) *Eur. J. Biochem.* 132, 531–536
- 14 Dalmark, M. and Wieth, J.O. (1972) *J. Physiol.* 224, 583–610
- 15 Funder, J. and Wieth, J.O. (1976) *J. Physiol.* 262, 679–698
- 16 Milanick, M.A. and Gunn, R.B. (1984) *Am. J. Physiol.* 247, C247–C259
- 17 Matsuyama, H., Kawano, Y. and Hamasaki, N. (1986) *J. Biochem.* 99, 496–501
- 18 Nigg, E., Kessler, M. and Cherry, R.J. (1979) *Biochim. Biophys. Acta* 550, 328–340
- 19 Chiba, T., Sato, Y. and Suzuki, Y. (1986) *Biochim. Biophys. Acta* 858, 107–117
- 20 Sato, Y., Chiba, T. and Suzuki, Y. (1986) *Biochim. Biophys. Acta* 856, 11–18
- 21 Cherry, R.J., Cogoli, A., Oppliger, M., Schneider, G. and Semenza, G. (1976) *Biochemistry* 15, 3653–3657
- 22 Good, N.E., Winget, G.D., Winter, W., Connolly, T.N., Azawa, S. and Singh, R.M.M. (1966) *Biochemistry* 5, 467–477
- 23 Dodge, J.T., Mitchell, C. and Hanahan, D.J. (1963) *Arch. Biochem. Biophys.* 100, 119–130
- 24 Lowry, O.H., Rosebrough, N.J., Farr, A.L. and Randall, R.J. (1951) *J. Biol. Chem.* 193, 265–275
- 25 Sato, Y., Chiba, T. and Suzuki, Y. (1985) *Chem. Pharm. Bull.* 33, 3935–3944
- 26 Lepke, S., Fasold, H., Pring, M. and Passow, H. (1976) *J. Membrane Biol.* 29, 147–177
- 27 Ship, S., Shami, Y., Breuer, W. and Rothstein, A. (1977) *J. Membrane Biol.* 33, 311–323
- 28 Brauer, M., Spread, C.Y., Reithmeier, R.A.F. and Sykes, B.D. (1985) *J. Biol. Chem.* 260, 11643–11650
- 29 Kampmann, L., Lepke, S., Fasold, H., Fritzsche, G. and Passow, H. (1982) *J. Membrane Biol.* 70, 199–216
- 30 Dalmark, M. (1976) *J. Gen. Physiol.* 67, 223–234
- 31 Cabantchik, Z.I. and Rothstein, A. (1972) *J. Membrane Biol.* 10, 311–330
- 32 Cabantchik, Z.I. and Rothstein, A. (1974) *J. Membrane Biol.* 15, 207–226
- 33 Frölich, O. (1982) *J. Membrane Biol.* 65, 111–123
- 34 Knauf, P.A., Ship, S., Breuer, W., McCulloch, L. and Rothstein, A. (1978) *J. Gen. Physiol.* 72, 607–630
- 35 Knauf, P.A., Breuer, W., McCulloch, L. and Rothstein, A. (1978) *J. Gen. Physiol.* 72, 631–649
- 36 Knauf, P.A., Law, F.-A., Tarshis, T. and Furuya, W. (1984) *J. Gen. Physiol.* 83, 683–701
- 37 Passow, H. (1986) *Rev. Physiol. Biochem. Pharmacol.* 103, 61–204
- 38 Grintstein, S., McCulloch, L. and Rothstein, A. (1979) *J. Gen. Physiol.* 73, 493–514
- 39 Passow, H., Fasold, H., Gartner, E.M., Legrum, B., Ruffing, W. and Zaki, L. (1980) *Ann. N.Y. Acad. Sci.* 341, 361–383
- 40 Furuya, W., Tarshis, T., Law, F.-Y. and Knauf, P.A. (1984) *J. Gen. Physiol.* 83, 657–681
- 41 Fröhlich, O., Leison, C. and Gunn, R.B. (1983) *J. Gen. Physiol.* 81, 127–152
- 42 Jennings, M.L. (1982) *J. Gen. Physiol.* 79, 169–185
- 43 Falke, J.J., Pace, R.J. and Chan, S.I. (1984) *J. Biol. Chem.* 259, 6481–6491
- 44 Wieth, J.O., Bjerrum, P.J., Brahm, J. and Andersen, O.S. (1982) *Tokai J. Exp. Clin. Med.* 7, 91–101
- 45 Jennings, M.L. (1982) *J. Biol. Chem.* 257, 7554–7559
- 46 Wieth, J.O. and Bjerrum, P.J. (1982) *J. Gen. Physiol.* 79, 253–282
- 47 Wieth, J.O., Bjerrum, P.J. and Borders, C.L. (1982) *J. Gen. Physiol.* 79, 283–312
- 48 Bjerrum, P.J., Wieth, J.O. and Borders, C.L. (1983) *J. Gen. Physiol.* 81, 453–484
- 49 Zaki, L. (1981) *Biochem. Biophys. Res. Commun.* 99, 243–251
- 50 Zaki, L. (1983) *Biochem. Biophys. Res. Commun.* 110, 616–624
- 51 Zaki, L. (1984) *FEBS Lett.* 169, 234–240
- 52 Zaki, L. and Julien, T. (1985) *Biochim. Biophys. Acta* 818, 325–332
- 53 Wieth, J.O., Andersen, O.S., Brahm, J., Bjerrum, P.J. and Borders, C.L. (1982) *Philos. Trans. R. Soc. Lond. B.* 299, 383–399